Blockade of cysteinyl leukotriene receptor 1 alleviates asthma by inhibiting bronchial epithelial cell apoptosis and activating the Nrf2 signaling pathway

XIANGJIE WU, YIQIONG CHEN, SUPING CHEN and YIPING LIN

Department of Pediatrics, School of Medicine, Jinhua Polytechnic, Jinhua, Zhejiang 321007, P.R. China

Received January 30, 2024; Accepted October 16, 2024

DOI: 10.3892/etm.2024.12780

Abstract. The therapeutic role of blockade of cysteinyl leukotriene receptor 1 (CysLTR1) in asthma has been previously studied. However, the effect of CysLTR1 blockade on bronchial epithelial cell apoptosis and the nuclear factor erythroid-derived 2-related factor 2 (Nrf2) signaling pathway remains unclear. The present study established an ovalbumin (OVA)-induced asthmatic rat model. Varying doses (1, 4 and 30 mg/kg) of montelukast sodium, a specific CysLTR1 antagonist, were used to inhibit CysLTR1 function in an asthmatic rat model. Reverse transcription-quantitative PCR was used to detect the expression levels of CysLTR1, NAD(P)H quinone oxidoreductase 1 (NQO1) and heme oxygenase 1 (HO-1). CysLTR1 and Nrf2 protein expression levels were determined using western blotting. Immunofluorescence assays were used to evaluate the relative fluorescence intensity of Nrf2 in rat lung tissues. Lung tissue histology was assessed through hematoxylin & eosin, alcian blue and periodic acid-Schiff and Masson's trichrome staining assays. The levels of IL-17, IL-4, serum IgE and the reduced/oxidized glutathione ratio were determined using ELISA assay kits. The number of inflammatory cells was analyzed using Wright-Giemsa staining. Bronchial epithelial cell apoptosis was measured using a TUNEL assay. The results indicated that OVA-induced inflammatory responses and increased eosinophil, lymphocyte and macrophage counts were significantly attenuated following blockade of CysLTR1. Downregulated expression of antioxidant genes NQO1 and HO-1 and the reduced GSH/GSSG ratio caused by OVA challenge were restored by blockade of CysLTR1. Additionally, CysLTR1 blockade also reduced collagen deposition, suppressed goblet cell hyperplasia and inhibited bronchial epithelial cell apoptosis in a rat model of asthma. Furthermore, it was demonstrated that the blockade of CysLTR1 could significantly increase Nrf2 expression. In conclusion, the blockade of CysLTR1 could alleviate asthma in an OVA-induced rat model by inhibiting bronchial epithelial cell apoptosis and activating the Nrf2 signaling pathway. These data may potentially provide a theoretical basis for future asthma therapy in a clinical setting.

Correspondence to: Dr Yiping Lin, Department of Pediatrics, School of Medicine, Jinhua Polytechnic, 888 Haitang West Road, Jinhua, Zhejiang 321007, P.R. China
E-mail: 15168757819@163.com

Abbreviations: CysLT, cysteinyl leukotriene; CysLTR1, CysLT receptor 1; OVA, ovalbumin; Nrf2, nuclear factor erythroid-derived 2-related factor 2; NQO1, NAD(P)H quinone oxidoreductase 1; HO-1, heme oxygenase 1; H&E, hematoxylin & eosin; BALF, bronchoalveolar lavage fluid

Key words: cysteinyl leukotriene 1 receptor, asthma, inflammation, nuclear factor erythroid 2-related factor 2, airway remodeling, apoptosis

Introduction

Asthma, a chronic and heterogeneous disease affecting the lower airways, is characterized by persistent inflammation and airway hyper-responsiveness, resulting in symptoms such as coughing, wheezing, dyspnea and chest tightness (1,2). The prevalence of asthma varies worldwide, ranging from 2.1% in Indonesia to 32.2% in the United Kingdom due to environmental differences (3). Based on extrapolation from existing data, the World Health Organization predicts a projected increase in the number of individuals with asthma by an additional 100 million up to 2025 (4). Therefore, the exploration of novel therapies and therapeutic targets is imperative to enhance symptom control and minimize exacerbations in patients with severe asthma.

The airway epithelium functions as the primary interface of the body with inhaled air and other substances, establishing the initial defense barrier against exogenous particles (5). Airway epithelial cells constitute the frontline defense against inflammatory stimuli and antigens, safeguarding the airways and lungs from exposure (6). Bronchial biopsies commonly exhibit shedding of bronchial epithelial cells, which is a significant histological characteristic of patients with asthma (7). A number of studies have reported an increased incidence of apoptosis in bronchial epithelial cells among adults with asthma (8,9). Research has shown that nuclear factor erythroid-derived 2-related factor 2 (Nrf2) is an essential endogenous transcription factor with antioxidant and antiapoptotic properties (10,11). In normal conditions, Nrf2 remains inactive in the cytoplasm while bound to its inhibitor, Kelch-like ECH associated protein 1 (Keap1) (12). However,

exposure to environmental stress triggers the activation of Nrf2 by separating it from Keap1. This leads to its translocation into the nucleus and subsequent stimulation of various genes responsible for antioxidant activity, such as NAD(P)H quinone oxidoreductase 1 (NQO1), heme oxygenase 1 (HO-1) and glutathione peroxidase (13). The Nrf2 signaling pathway serves a crucial role in protecting individuals with asthma and maintaining the integrity of bronchial epithelial barriers (14). Additionally, studies have reported that activating Nrf2 can inhibit apoptosis in bronchial epithelial cells, reduce airway inflammation, alleviate airway hyper-responsiveness and mitigate oxidative stress in mouse models of asthma (15-17). Therefore, gaining a deeper understanding of airway epithelial apoptosis and activation of the Nrf2 signaling pathway may uncover novel therapeutic approaches for managing asthma.

Long-acting β2 agonists and inhaled corticosteroids are commonly used as bronchodilators and anti-inflammatory agents in the treatment of asthma (18). However, the use of these drugs can lead to numerous side effects, such as dysphonia, xerostomia, adrenal insufficiency and osteoporosis (19). Cysteinyl leukotrienes (CysLTs) are a group of lipid mediators that exhibit proinflammatory activities and cause constriction of the bronchi during allergic inflammation (20). A number of studies have reported the presence of elevated levels of CysLTs in the urine or exhaled air condensate from individuals with asthma (21,22). The majority of the effects induced by CysLTs, which are relevant to the pathophysiology of asthma, are mediated through the activation of CysLT receptor 1 (CysLTR1) (23). This receptor was among the first specific mediators successfully targeted for drug development against asthma symptoms (24). Consequently, CysLTR1 antagonists are considered alternative medications for treating asthma effectively (25), resulting in the widespread use of prescription drugs targeting CysLTR1 (26-28). Montelukast sodium, a CysLTR1-specific antagonist, has shown efficacy in reducing pulmonary fibrosis, airway hyper-responsiveness and inflammation in mouse models of asthma (29,30). However, the effects of CysLTR1 blockade on bronchial epithelial cell apoptosis and the Nrf2 signaling pathway during asthma progression are currently poorly understood.

In the present study, an ovalbumin (OVA)-induced asthmatic rat model was established. The effects of different doses of montelukast sodium on bronchial epithelial cell apoptosis and the Nrf2 signaling pathway in asthma progression were investigated. These results may further clarify the role of CysLTR1 on the progression of asthma and expand our understanding of the protective mechanism of CysLTR1 antagonists in asthma pathogenesis.

Materials and methods

Reagents. Montelukast sodium, OVA (grade V) and bovine serum albumin (BSA) were purchased from MilliporeSigma. Aluminum hydroxide gels were purchased from Thermo Fisher Scientific, Inc. The alcian blue & periodic acid-Schiff (AB-PAS) staining kit and TUNEL cell apoptosis kit were purchased from Solarbio Science & Technology Co., Ltd. The Masson's trichrome staining kit was purchased from Maxim Biotech, Inc. The hematoxylin & eosin (H&E) staining kit and Wright-Giemsa stain kit were purchased from Abcam. Primary antibodies targeting CysLTR1 (cat. no. 27372-1-AP), Nrf2 (cat. no. 16396-1-AP) and GAPDH (cat. no. 60004-1-Ig) were purchased from Proteintech Group. Inc. The RIPA lysis buffer was purchased from Wuhan Boster Biological Technology, Ltd. The ECL reagent was purchased from Tanon Science and Technology Co., Ltd. and the BCA reagent was purchased from Thermo Fisher Scientific, Inc. The Rat IgE ELISA kit (cat. no. EKF58258) was purchased from Biomatik. The Rat IL-17 (cat. no. KTE9005) and IL-4 (cat. no. KTE9003) ELISA kits as well as HRP-conjugated secondary antibodies (cat. nos. A21020 and A21010) were purchased from Abbkine Scientific Co., Ltd. The reduced glutathione (GSH)/oxidized glutathione (GSSG) Ratio Fluorometric Detection Assay Kit (cat. no. 50120ES70) was purchased from Shanghai Yeasen Biotechnology Co., Ltd. The total RNA extraction kit (cat. no. LS1040) was purchased from Promega Corporation. The First Strand Kit and QuantiFast SYBR® Green PCR Kit were purchased from Qiagen GmbH.

Animal grouping and treatment. A total of 30 Sprague-Dawley male rats (age, 8-10 weeks) weighing 240±5 g, were purchased from Beijing Vital River Laboratory Animal Technology Co., Ltd. All rats were housed in specific pathogen free cages under standard laboratory conditions, which included a temperature of 22-25˚C, a relative humidity of 40-55% and a 12/12 h light/dark cycle with free access to water and food. Following acclimation, the rats were randomly assigned to five treatment groups: i) The control (Group I); ii) model (Group II); iii) low-dose (1 mg/kg) montelukast sodium (Group III); iv) medium-dose (4 mg/kg) montelukast sodium (Group IV); and v) high-dose (30 mg/kg) montelukast sodium (Group V) groups, with 6 rats/group. OVA was dissolved in 4% aluminum hydroxide gels to prepare an OVA solution (2 mg/ml). The OVA-induced asthmatic rat model was established as previously described (31,32) with some amendments. On days 0 and 14, rats in Groups II-V were sensitized with an intraperitoneal injection of OVA solution (0.5 ml/rat). Rats in Group I were administered an equal volume of saline. From the 15th day, all rats apart from the control group, were administered with inhaled OVA aerosol (10 mg/ml; dissolved in saline; 30 min/day) for 3 weeks. Before the OVA challenge (from the 15th day onwards), rats in Group I and II were given 10 ml/kg/day of saline by gavage, while rats in Groups III-V were given montelukast sodium by gavage at doses of 1, 4 and 30 mg/kg/day, respectively. The gavage procedures were continuously conducted until sample collection. The experiment duration was 5 weeks. The heart rate of the animals was monitored each day using a polyethylene cannula (PE 50) filled with heparinized saline (100 IU/ml) inserted into the right carotid artery. The cannula was connected to a transducer, and the signal was amplified by bioamplifier and an acquisition data system (AD Instruments Pvt. Ltd. with software LabChart 7.3; AD Instrument Pvt. Ltd). Body weight was monitored each week. Throughout the experiment, the aim was to minimize the utilization of animals and alleviate their distress as much as possible. According to the analgesic methods described in previous studies, intraperitoneal injection of 5 mg/kg tramadol has been reported to be a safe and effective analgesic in rats and mice (33,34). In preliminary experiments, 5 mg/kg tramadol was found to effectively alleviate pain in rats without

any side effects or mortality (data not shown). Therefore, 5 weeks later, all animals received an intraperitoneal injection of tramadol (5 mg/kg) as an analgesic method to minimize pain, suffering and distress. The rats were housed individually in a polycarbonate cage and allowed to recover on a heating pad to maintain a body temperature of 37.5±0.5˚C. In addition, the rats were monitored for any signs of fatigue and stress. Researchers were trained to apply the humane endpoints, if any animal exhibited features of a compromised welfare. The humane endpoints included rapid weight loss (>20% of normal body weight) and/or rapid or labored breathing. No animals died naturally during the experiments and all of the rats were euthanized by an intraperitoneal injection of pentobarbital sodium overdose (200 mg/kg) on day 35. Death was confirmed by cardiac and respiratory arrest and a lack of response to tail clamping. The bronchoalveolar fluid lavage (BALF) was obtained by washing the lungs and subsequent analysis involved the collection of lung tissues and airway tissues. To analyze the level of OVA-specific IgE in serum, blood samples (300 μl) were collected from rats by cardiac puncture. Whole blood was collected and left to coagulate at room temperature for at least 30 min, and then centrifuged at 1,000 x g for 10 min at 4˚C. The serum samples were stored at -20˚C until use. The experiments in the present study were carried out by three skilled technicians who were unaware of the experimental design and purpose. Animal experiments followed the guidelines provided by the National Institutes of Health Guide for the Care and Use of Laboratory Animals and received approval from the Ethics Committee of Jinhua Polytechnic (approval no. 20221221; Jinhua, China).

Histopathologic examination. The airway tissues were fixed using 4% paraformaldehyde (48 h; 4˚C), embedded in paraffin and cut into 5-μm sections. Subsequently, sections were stained with hematoxylin for 5 min and eosin for 2 min at room temperature using a H&E staining kit. Masson's staining was performed using a Masson's trichrome staining kit in accordance with the manufacturer's protocol to observe collagen deposition at room temperature for a total of 15 min (Wiegert's iron hematoxylin, 8 min; Biebrich scarlet, 5 min; aniline blue, 2 min) at room temperature. Based on the manufacturer's protocol of the AB-PAS staining kit, sections were stained with alcian blue for 30 min and periodic acid Schiff for 15 min at room temperature. The pathological structure of airway tissues was observed using a BX53 light microscope (Olympus Corporation).

ELISA and biochemical assays. According to the manufacturer's instructions, the GSH/GSSG ratio, levels of IL-4 and IL-17 in lung tissues and serum IgE concentration were determined using corresponding commercial kits (35).

Total RNA isolation and reverse transcription-quantitative PCR (RT-qPCR). Total RNA from lung tissues was extracted using a total RNA extraction kit. The concentration of total RNA was measured using a NanoDrop™ 2000 spectrophotometer (Thermo Fisher Scientific, Inc.). Total RNA (500 ng) was reverse transcribed into cDNA at 42˚C for 45 min using a First Strand Kit and RT-qPCR was performed using the QuantiFast SYBR® Green PCR Kit, according to the manufacturer's instructions. The following thermocycling conditions were used for the qPCR: Initial denaturation at 95˚C for 3 min; followed by 40 cycles of denaturation at 95˚C for 15 sec, annealing at 60˚C for 30 sec and elongation at 72˚C for 1 min, as well as a final extension at 72˚C for 5 min. To determine gene expression levels, the $2^{-\Delta\Delta Cq}$ method was used (36) and results were normalized to GAPDH as a reference gene (37). The primer sequences used are presented in Table I.

Table I. Primers used for reverse transcription-quantitative PCR.

Gene	Sequence (5'-3')
Cysteinyl leukotriene receptor 1	F: CAAATGTGCCATGCCCTGAC
	R: GGTCCACTCCATTCACAGGG
NAD(P)H quinone oxidoreductase 1	F: AGCGCTTGACACTACGATCC
	R: TCTGCGTGGGCCAATACAAT
Heme oxygenase 1	F: ATGCCCCACTCTACTTCCCT
	R: TACGTAGTGCTGTGTGGCTG
GAPDH	F: ACTCCCATTCTTCCACCTTTG
	R: CCCTGTTGCTGTAGCCATATT

F, forward; R, reverse.

BALF analysis. The BALF samples were stained using a Wright-Giemsa stain kit, and the eosinophil, lymphocyte and macrophage counts were recorded under a light microscope (Olympus Corporation) and analyzed using Image-Pro-Plus (version 6.0; Media Cybernetics). The inhibitory activity (%) was evaluated as the following formula: (1-A/B) x100%. A represents the number of inflammatory cells in different groups of montelukast sodium; B represents the number of inflammatory cells in the model group.

Immunofluorescence assays. Lung tissue sections (5 μm) underwent deparaffinization in xylene for 10 min at room temperature and rehydration with descending concentrations of ethanol (100, 95 and 70% for 3-5 min each), followed by antigen retrieval in heated citrate buffer (10 mM; pH 6.0) at 80˚C for 25 min. Subsequently, the samples were washed three times with PBS before being permeabilized using 0.5% TritonX-100 in PBS. The sections were then blocked with 5% BSA at room temperature for 1 h. Next, the samples were incubated with primary antibodies against Nrf2 (1:50) overnight at 4˚C and the corresponding secondary antibodies (1:200) for 2 h at room temperature. Finally, after staining with DAPI (1 μg/ml) at room temperature for 15 min, the samples were imaged using a fluorescence microscope (Olympus Corporation). Image-Pro-Plus (version 6.0; Media Cybernetics) was adopted to analyze the fluorescence intensity.

TUNEL assay. Apoptosis of lung tissues was determined in accordance with the experimental procedures outlined in the manufacturer's guidelines for the TUNEL kit. In brief, the lung tissues were fixed using 4% paraformaldehyde (48 h; 4˚C), embedded in paraffin and cut into 5-μm sections. The deparaffinized tissue sections were incubated with 3% hydrogen

peroxide in methanol for 10 min at 25˚C in the dark, washed three times with PBS and incubated with 0.1% Triton X-100 in freshly prepared 0.01% sodium citrate for 8 min at 25˚C. Tissue sections were then incubated with proteinase K working solution for 25 min at 37˚C and washed three times with PBS (pH 7.4) for 5 min each. A total of 50 μl TUNEL reagent was added to each sample and incubated at 37˚C for 60 min. The sections were washed three times with PBS (pH 7.4) and then cell nuclei were counterstained with 2 μg/ml DAPI solution at room temperature for 10 min in the dark and mounted with 50 μl anti-fade mounting medium. TUNEL-positive cells were observed in five randomly-selected fields using a fluorescence microscope (Olympus Corporation) and analyzed using Image-Pro-Plus (version 6.0; Media Cybernetics).

Western blot analysis. The RIPA lysis buffer was employed for the extraction of total proteins from lung tissues, followed by quantification using a BCA kit. Subsequently, a total of 50 μg of protein/lane was separated by 10% SDS-PAGE and proteins then were transferred to polyvinylidene fluoride membranes. Following blocking with 5% nonfat milk for 2 h at 25˚C, membranes were incubated with primary antibodies against CysLTR1 (1:4,000), Nrf2 (1:7,000) and GAPDH (1:50,000) overnight at 4˚C. Then, tris-buffered saline with 0.05% Tween-20 was used to wash the membranes three times. Subsequently, at room temperature, the HRP-conjugated secondary antibodies (1:10,000) were incubated with samples for 1 h. The signals were detected using an ECL kit (Beyotime Institute of Biotechnology) and blots were quantified under a Gel-Proanalyzer (version 4.0; Media Cybernetics). GAPDH was used as the loading control (38).

Statistical analysis. Data were analyzed using one-way ANOVA, followed by Tukey's post-hoc test. Data analysis was performed using SPSS software (version 22.0; IBM Corp.). The data are presented as the mean ± standard deviation. P<0.05 was considered to indicate a statistically significant difference.

Results

Blockade of CysLTR1 alleviates inflammation in asthmatic rats through Nrf2. The heart rate and body weight of rats were monitored throughout the study. The results demonstrated a significant decrease in the heart rate of the model group compared with that in the control group (Fig. 1A; P<0.001). Administration of montelukast sodium significantly increased the heart rate of rats at all doses tested, compared with that in the model group (P<0.001). From day 21, a significant decrease in body weight was observed in the model group compared with the control group (Fig. 1B; P<0.05); however, administration of montelukast sodium significantly restored the body weight of asthmatic rats from the 28th day onwards (P<0.05).

Following administration of different doses of montelukast sodium, the mRNA and protein expression levels of CysLTR1 in lung tissues were measured. The model group demonstrated a significant increase in both the mRNA and protein expression levels of CysLTR1 compared with that of the control group (Fig. 1C; P<0.001). Moreover, it was demonstrated that, compared with the model group, administration of montelukast sodium significantly reduced the mRNA expression level of CysLTR1 to varying degrees (P<0.05); however, only administration of the medium-dose montelukast sodium decreased the protein expression level of CysLTR1 significantly compared with that in the model group (Fig. 1D; P<0.05). On the contrary, a significant decrease in the protein expression level of Nrf2 was observed in the model group compared with that in the control group (P<0.001), while all doses of montelukast sodium significantly increased the Nrf2 protein expression level, with the higher increase being observed at a dosage of 4 mg/kg (P<0.001).

H&E staining was performed to assess the impact of CysLTR1 blockade on inflammation in rat lung tissues. No apparent inflammatory cell infiltration was observed in the control group, while the model group demonstrated a noticeable infiltration of inflammatory cells and visible thickening of smooth muscle layers compared with the control group (Fig. 1E). Compared with the model group, the administration of montelukast sodium, particularly at a dosage of 4 mg/kg, reduced inflammatory infiltration and airway remodeling. Upon OVA challenge, a significant increase in IL-17 and IL-4 levels in the model group were observed compared with those in the control group, which was consistent with the H&E staining data (Fig. 1F; P<0.001). Furthermore, treatment with montelukast sodium significantly mitigated the proinflammatory effects induced by OVA challenge (P<0.05). IgE is reported to have evolved in mammals as a primary defense mechanism against pathogens, and increased IgE levels are considered indicative of an increased susceptibility to the development of asthma (39). It was demonstrated that IgE concentration was significantly increased in the model group compared with that in the control group (Fig. 1G; P<0.001), while the administration of montelukast sodium was effective in decreasing IgE levels (P<0.01). Additionally, due to the strong association of eosinophils, lymphocytes and macrophages with inflammatory processes in asthma (40), cell count analysis was performed on BALF samples from asthmatic rats. The results of Wright-Giemsa staining demonstrated that the model group exhibited a significant increase in the numbers of eosinophils, lymphocytes and macrophages, compared with those in the control group (Fig. 1H; P<0.001). Administration of montelukast sodium significantly decreased the elevated cell counts in the BALF of asthmatic rats induced by OVA challenge (P<0.05). The association between the dose of montelukast sodium and changes in the number of these inflammatory cells was then assessed. It was observed that varying dosages of montelukast sodium exhibited the lowest inhibitory activity on eosinophils and the highest inhibitory activity on macrophages. Moreover, among the three doses of montelukast sodium tested, the 4 mg/kg dose demonstrated the largest inhibitory efficacy across all three types of inflammatory cells.

Blockade of CysLTR1 attenuates airway remodeling in asthmatic rats. The hyperplasia of goblet cells and the deposition of collagen in the lungs are crucial indicators for the progression of asthma (41,42). The model group of rats demonstrated marked goblet cell hyperplasia in comparison with the control group (Fig. 2A). However, the montelukast sodium-treated groups showed a decreased degree of goblet

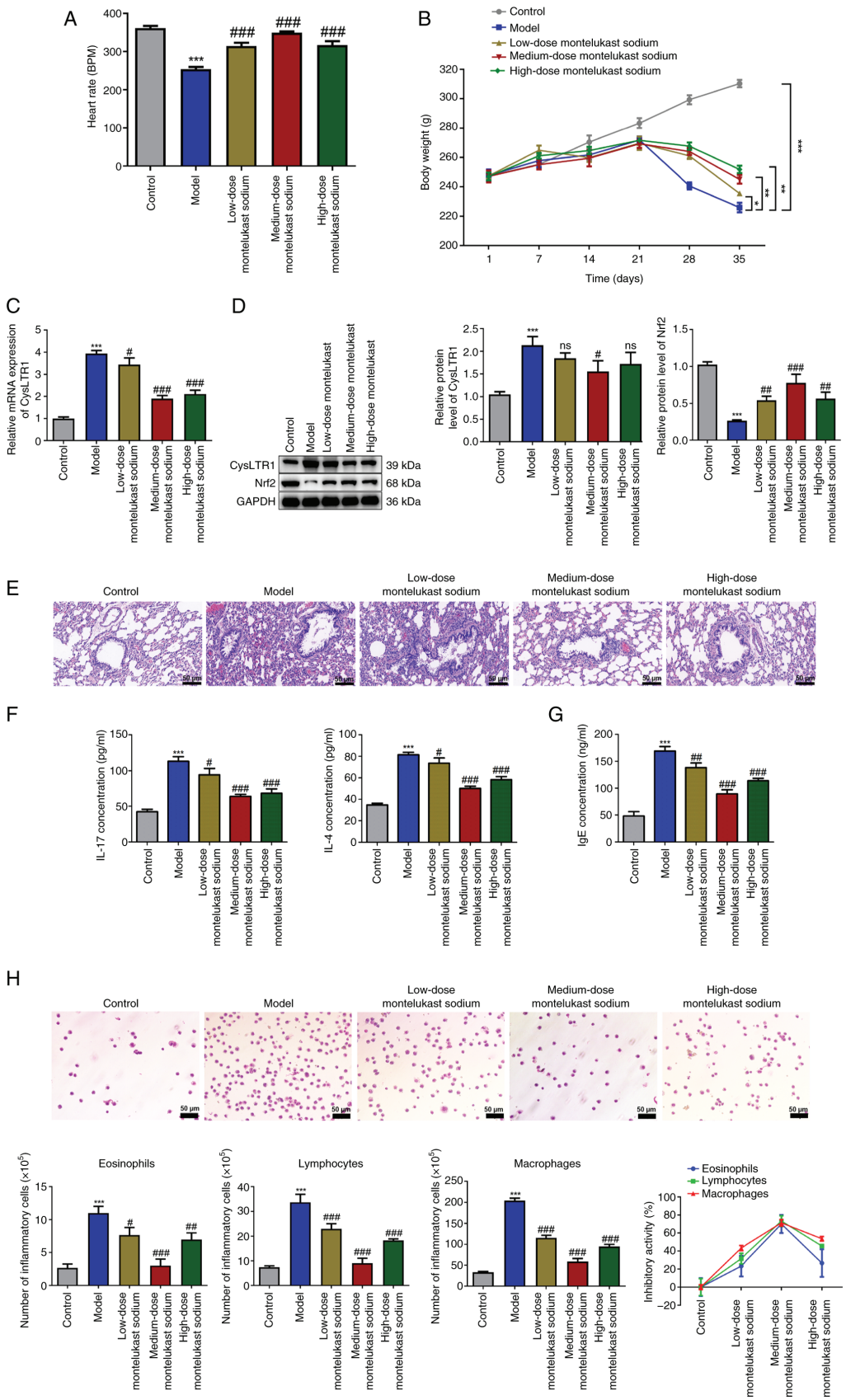

Figure 1. Blockade of CysLTR1 alleviates inflammation in asthmatic rats. (A) Heart rate and (B) body weight of different groups of rats treated with montelukast sodium. *P<0.05, **P<0.01, ***P<0.001. (C) mRNA expression levels of CysLTR1 in lung tissues were determined using reverse transcription-quantitative PCR. (D) Protein expression levels of CysLTR1 and Nrf2 in lung tissues were determined by western blotting. (E) The histopathological changes in lung tissues from different groups of rats treated with montelukast sodium were assessed by hematoxylin and eosin staining (scale bar, 50 μm). (F) Expression levels of IL-17 and IL-4 in the lung and (G) serum IgE were determined by ELISA. (H) Numbers of inflammatory cells in bronchoalveolar lavage fluid were measured by Wright-Giemsa staining and the association between the dose of montelukast sodium and changes in the number of lymphocytes, eosinophils and macrophages was assessed (scale bar, 50 μm). ***P<0.001 vs. control; #P<0.05, ##P<0.01 and ###P<0.001 vs. model. ns, not significant; BPM, beats per minute; Nrf2, nuclear factor erythroid-derived 2-related factor 2; CysLTR1, cysteinyl leukotriene receptor 1.

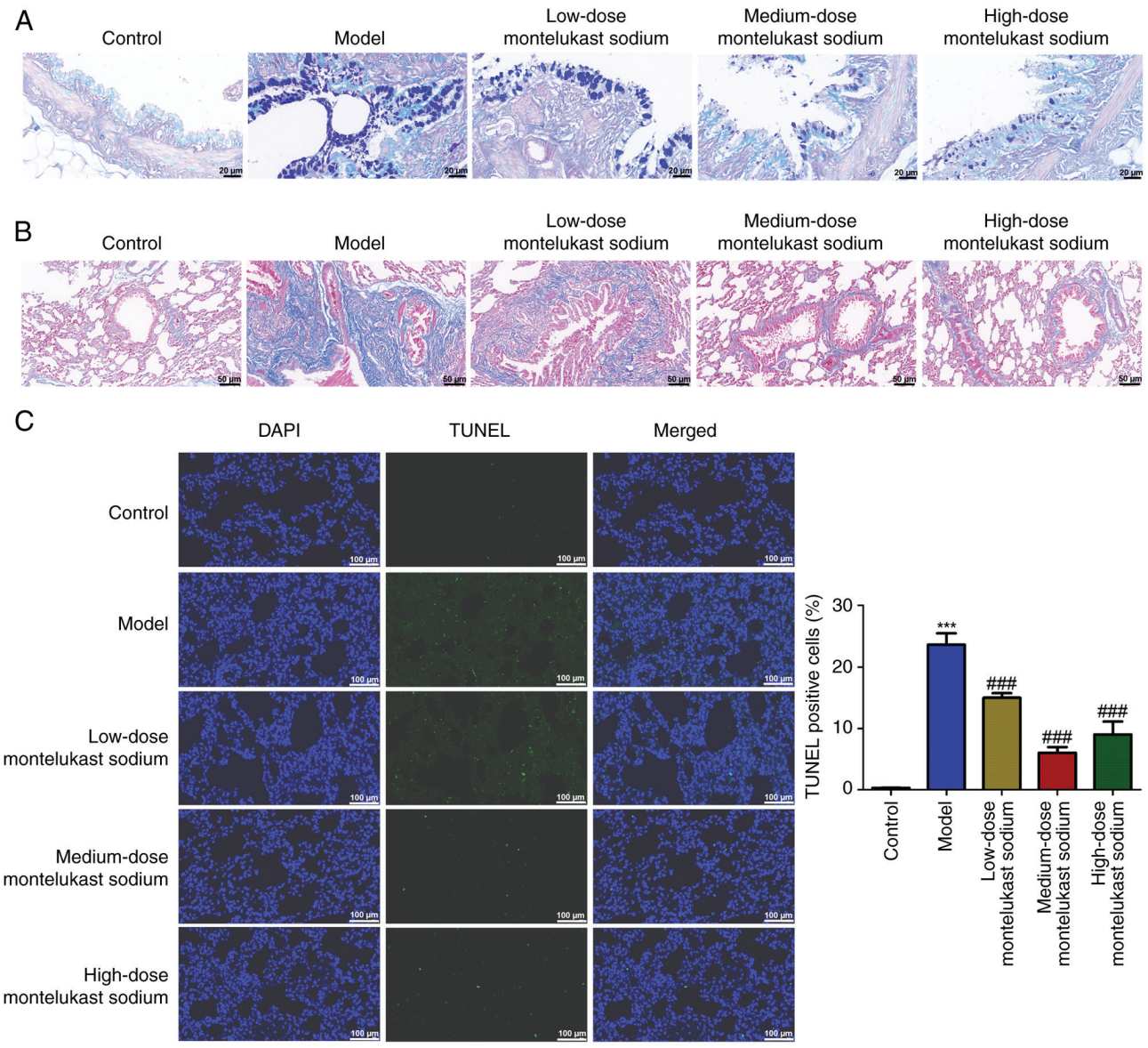

Figure 2. Blockade of cysteinyl leukotriene receptor 1 attenuates airway remodeling in asthmatic rats. (A) Goblet cell hyperplasia was measured by alcian blue & periodic acid-Schiff staining (scale bar, 20 μm). (B) The collagen deposition in lung tissues from each group was assessed by Masson's trichrome staining (scale bar, 50 μm). (C) The apoptosis of bronchial epithelial cells was determined by TUNEL assay (scale bar, 100 μm). ***P<0.001 vs. control; $^{###}$P<0.001 vs. model.

cell hyperplasia compared with that in the model group (Fig. 2A). Additionally, the asthmatic rat model exhibited an exacerbation of OVA-induced collagen deposition in the lung tissue; however, treatment with montelukast sodium mitigated these changes. A TUNEL assay was used to examine the impact of montelukast sodium on bronchial epithelial cell apoptosis. The number of TUNEL-positive cells in the model group was significantly increased compared with that in the control group (Fig. 2C; P<0.001), whereas the number of TUNEL-positive cells was significantly reduced by the administration of montelukast sodium, compared with that in the model group (P<0.001).

Blockade of CysLTR1 inhibits oxidative stress and activates Nrf2 in asthmatic rats. The expression levels of antioxidant genes NQO1 and HO-1 were measured to investigate the involvement of CysLTR1 blockade in oxidative stress. Additionally, the GSH/GSSG ratio was calculated, due to its reported role in scavenging free radicals (43). A significant decrease in the mRNA expression levels of NQO1 and HO-1 was demonstrated in the model group compared with those in the control group (Fig. 3A and B; P<0.001). Additionally, a significant reduction in the GSH/GSSG ratio was also demonstrated (Fig. 3C; P<0.001). These inhibitory effects induced by OVA challenge were reversed by treatment with montelukast sodium, particularly at a dosage of 4 mg/kg (Fig. 3A-C; P<0.001). The transcription factor Nrf2, which is responsible for regulating cellular redox balance and initiating protective antioxidant responses in mammals, has been reported to be an important therapeutic target for mitigating oxidative stress injury in asthma (44). Immunofluorescence microscopy demonstrated a significant decrease in Nrf2 fluorescence intensity in the model group compared with that in the control group (Fig. 3D; P<0.001), while there was a significant increase

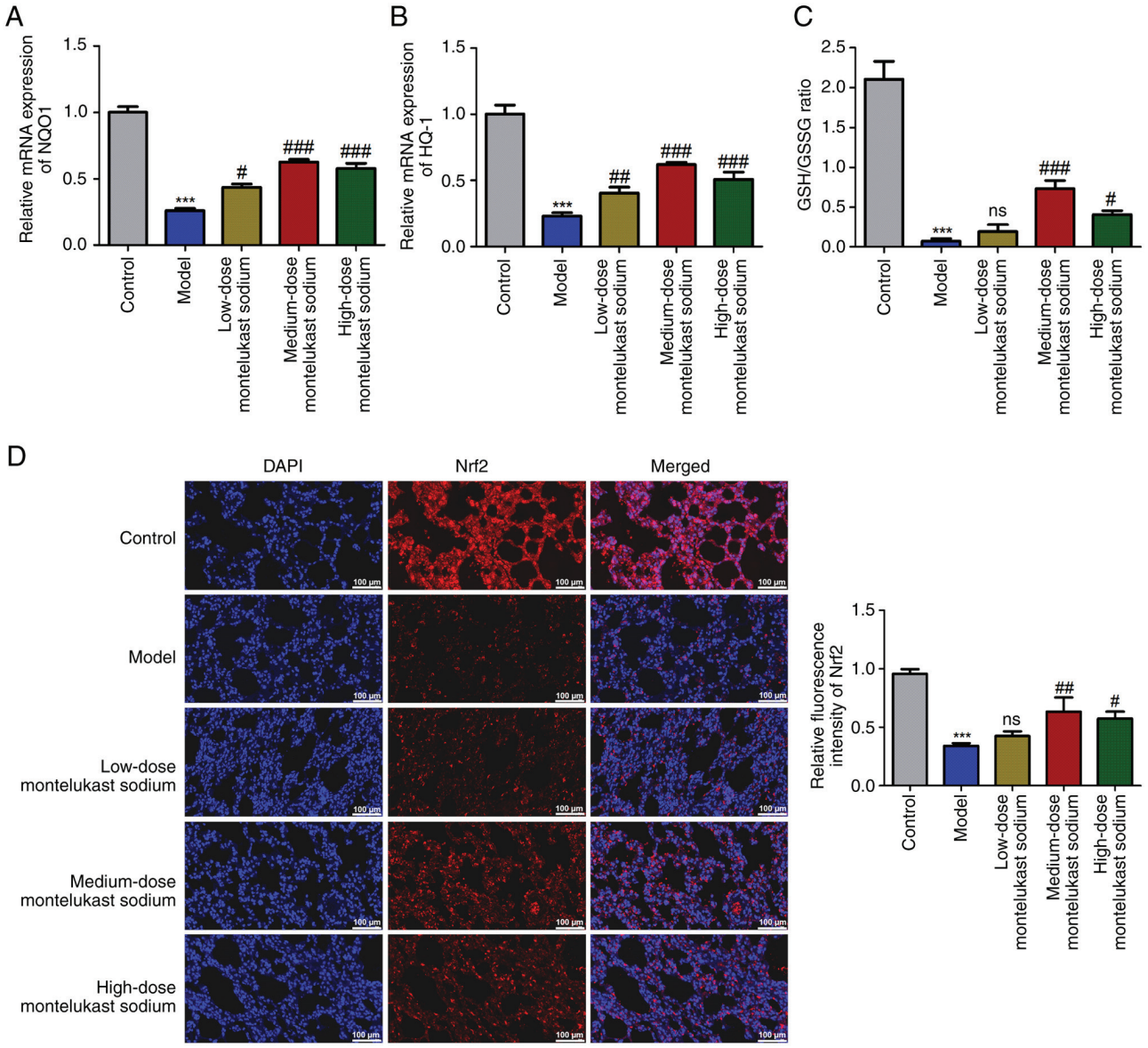

Figure 3. Blockade of cysteinyl leukotriene receptor 1 inhibits oxidative stress and activates Nrf2 signaling in asthmatic rats. The mRNA expression levels of (A) NQO1 and (B) HO-1 in lung tissues from each group were detected using reverse transcription-quantitative PCR. (C) The GSH/GSSG ratio was determined using a commercial assay kit. (D) Relative fluorescence intensity of Nrf2 in lung tissues was assessed by immunofluorescence microscopy (scale bar, 100 μm). ***P<0.001 vs. control; $^{\#}$P<0.05, $^{\#\#}$P<0.01 and $^{\#\#\#}$P<0.001 vs. model. ns, not significant; Nrf2, nuclear factor erythroid-derived 2-related factor 2; NQO1, NAD(P)H quinone oxidoreductase 1; HO-1, heme oxygenase 1; GSH, reduced glutathione; GSSG, oxidized glutathione.

following treatment with 4 or 30 mg/kg montelukast sodium (Fig. 3D; P<0.05).

Discussion

The prevalence of asthma has increased over recent decades, concomitant with the process of urbanization and industrialization (45). Despite strict adherence to prescribed anti-asthma medication, certain patients with asthma continue to experience uncontrolled clinical symptoms, indicating an ongoing need for effective management (46). Medical care and excessive absenteeism related to asthma lead to substantial healthcare expenditures exceeding $80 billion annually, including $50.3 billion in direct medical costs, $29 billion in asthma-related mortality and $3 billion in absenteeism (47). Therefore, despite the current availability of innovative therapies and evidence-based care, asthma continues to pose a significant public health challenge. The present study aimed to further elucidate the mechanism of action of CysLTR1 in the progression of asthma *in vivo*, and the results indicated that blockade of CysLTR1 may mitigate asthma progression in an asthmatic rat model by inhibiting bronchial epithelial cell apoptosis and activating Nrf2 signaling.

OVA challenge is a sensitization method used to induce asthma in murine models (48). In the present study, the pathological tissue of asthmatic rats exhibited noticeable infiltration of inflammatory cells and visible thickening of smooth muscle layers. Furthermore, elevated levels of inflammatory cytokines IL-17 and IL-4 were also observed in asthmatic rats. Inflammatory cells, such as macrophages, lymphocytes and eosinophils, have previously been reported to be closely associated with the inflammatory processes

in asthma (40,49). Eosinophilic airway inflammation is a defining characteristic of disease severity in specific subsets of individuals with severe asthma, and there is a direct association between eosinophil count and the frequency of asthma exacerbation (50-52). In the present study, a significant increase in the cell counts of macrophages, lymphocytes and eosinophils in the BALF of asthma rats were demonstrated. High levels of IgE are considered a biological indicator of increased susceptibility to the development of asthma (39). Furthermore, a previous study showed significant specific IgE sensitization in a number of patients, particularly among young individuals with severe forms of asthma (53). Additionally, the relative importance of IgE compared with eosinophils in severe asthma has also been reported, indicating that IgE is the main cause of allergic asthma, while eosinophilia is a consequence of the overall process (54). Similarly, the present study demonstrated a significant increase in IgE levels in asthmatic rats compared with control rats. The present results were consistent with the inflammatory characteristics of asthma, indicating the successful establishment of an asthmatic model in rats.

CysLTs, a crucial group of inflammatory mediators in the pathophysiology of asthma, are generated by activated macrophages, basophils, eosinophils, myeloid dendritic cells and mast cells (55). The above immune cells exert proinflammatory effects by specifically binding to CysLTR1 (56). Thus, antagonism of their actions produces anti-inflammatory properties. In the present study, montelukast sodium, a specific CysLTR1 antagonist, was used to block CysLTR1 and the role of CysLTR1 blockade on inflammatory responses during the progression of asthma was explored. Previous studies have reported that when the dosage of montelukast sodium is <1 mg/kg, there is no significant improvement in inflammation (57,58); however, when the dosage is ≥3 mg/kg, it can significantly reduce airway remodeling and inflammation (59,60). Additionally, it has also been reported that a single high dose of montelukast sodium (≥30 mg/kg) can alleviate inflammatory symptoms in animal models of asthma (61). Therefore, in the present study, low (1 mg/kg), medium (4 mg/kg) and high doses (30 mg/kg) of montelukast sodium were administered to rat models with asthma. Blockade of CysLTR1, particularly at the dose of 4 mg/kg of montelukast sodium, significantly attenuated the inflammatory symptoms and inflammatory cytokine levels in asthmatic rats. Additionally, blockade of CysLTR1 also suppressed the number of eosinophils, lymphocytes and macrophages in the BALF of asthmatic rats. Among the three dosages of montelukast sodium tested, the 4 mg/kg dose demonstrated the highest inhibitory capacity across all three types of inflammatory cells. These results suggested that blockade of CysLTR1 may confer protection against inflammatory infiltration in asthma progression. The specific binding of CysLTs to CysLTR1 not only mediates the inflammatory response in the progression of asthma, but also exerts a significant impact on airway remodeling (62). The present study demonstrated that the blockade of CysLTR1 significantly attenuated OVA-induced goblet cell hyperplasia and collagen deposition, which indicated its potential role in alleviating airway remodeling in asthmatic rats. It has been reported that the apoptosis and shedding of bronchial epithelial cells are significant histological characteristics in the development of asthma (63). Therefore, the present study investigated the role of CysLTR1 blockade on bronchial epithelial cell apoptosis through the TUNEL assay. These results demonstrated that the blockade of CysLTR1 decreased the percentage of TUNEL-positive cells in asthmatic rats, indicating the potential suppressive role of CysLTR1 blockade on the apoptosis of bronchial epithelial cells. However, there are a number of limitations in measuring the rate of apoptosis. First, other techniques, such as flow cytometry and transmission electron microscopy, are also available for measuring apoptosis. Second, previous studies have reported that in allergies with an inflammatory component, apoptosis is induced by proinflammatory mediators, such as TNF-α, produced by inflammatory cells (64) and TNF-α expression is strongly associated with the number of inflammatory cells present in inflammatory reactions (65). Moreover, TNF-α-induced cells have been shown by transmission electron microscopy to exhibit features characteristic of the early and advanced stages of apoptotic cell death, such as condensation of chromatin at the nuclear periphery, fragmentation of nuclei and formation of apoptotic bodies (66). Therefore, the expression levels of TNF-α and the associations between TNF-α and inflammatory cell numbers should be assessed in future studies. Collectively, blockade of CysLTR1 could potentially alleviate the development of asthma through inhibiting inflammation, airway remodeling and bronchial epithelial cell apoptosis.

It has been reported that the dysregulation of antioxidant and oxidant systems can expedite the exacerbation of asthma (67). Nrf2 regulates the encoding of antioxidant proteins through its interaction with antioxidant response elements, making it the foremost endogenous pathway for combating oxidative stress reported to date. HO-1 and NQO1 are the two most important antioxidant genes downstream of the Nrf2 pathway (68). HO-1 safeguards cellular integrity by suppressing oxidative stress and maintaining mitochondrial function, while NQO1 directly scavenges superoxide and contributes to the production of antioxidant forms (69,70). Thus, the present study determined the expression levels of Nrf2, HO-1 and NQO1 in asthmatic rats. The oxidative stress damage during asthma development led to the inhibition of the antioxidant genes Nrf2, HO-1 and NQO1 in asthmatic rats. Furthermore, the GSH/GSSG ratio, which is another major determinant of oxidative stress, was also suppressed following OVA challenge. Additionally, blockade of CysLTR1, particularly at a dosage of 4 mg/kg, restored the expression levels of Nrf2, NQO1 and HO-1 and the GSG/GSSG ratio in asthmatic rats. These findings suggested that blockade of CysLTR1 could activate the Nrf2 signaling pathway to inhibit oxidative stress and affect asthma progression.

In conclusion, the present study analysed the potential of CysLTR1 blockade in asthma pathogenesis, indicating that it could effectively suppress inflammation, airway remodeling, bronchial epithelial cell apoptosis and oxidative stress to improve asthma, potentially by activating the Nrf2 signaling pathway. This may provide valuable insights for future potential clinical therapeutic interventions for asthma.

Acknowledgements

Not applicable.

Funding

The present study was supported by the Science and Technology Plan Project in Jinhua City (grant nos. 2021-3-153 and 2022-4-028) and the Applied Research of Public Welfare Technology Foundation of Zhejiang Province (grant no. LGF21H010002).

Availability of data and materials

The data generated in the present study may be requested from the corresponding author.

Authors' contributions

YL made substantial contributions to the conception and design of the study. XW, YC and SC made substantial contributions to the acquisition, analysis and interpretation of the data. XW drafted the manuscript. All authors critically revised the manuscript for intellectual content. XW, YC and SC confirm the authenticity of all the raw data. All authors read and approved the final manuscript.

Ethics approval and consent to participate

All experimental procedures were conducted in compliance with the Guidelines for Care and Use of Laboratory Animals of the National Institutes of Health and were approved by the Ethics Committee of Jinhua Polytechnic (approval no. 20221221; Jinhua, China).

Patient consent for publication

Not applicable.

Competing interests

The authors declare that they have no competing interests.

References

1. Cevhertas L, Ogulur I, Maurer DJ, Burla D, Ding M, Jansen K, Koch J, Liu C, Ma S, Mitamura Y, *et al*: Advances and recent developments in asthma in 2020. Allergy 75: 3124-3146, 2020.
2. Poon AH and Hamid Q: Severe Asthma: Have we made progress? Ann Am Thorac Soc 13 (Suppl 1): S68-S77, 2016.
3. Stern J, Pier J and Litonjua AA: Asthma epidemiology and risk factors. Semin Immunopathol 42: 5-15, 2020.
4. GBD 2019 Chronic Respiratory Diseases Collaborators: Global burden of chronic respiratory diseases and risk factors, 1990-2019: An update from the Global Burden of Disease Study 2019. EClinicalMedicine 59: 101936, 2023.
5. Weinstock J, Chen XX, Nino G, Koumbourlis A and Rastogi D: The interplay between airway epithelium and the immune system-A primer for the respiratory clinician. Paediatr Respir Rev 38: 2-8, 2021.
6. Miller RL, Grayson MH and Strothman K: Advances in asthma: New understandings of asthma's natural history, risk factors, underlying mechanisms, and clinical management. J Allergy Clin Immunol 148: 1430-1441, 2021.
7. Yang Y, Jia M, Ou Y, Adcock IM and Yao X: Mechanisms and biomarkers of airway epithelial cell damage in asthma: A review. Clin Respir J 15: 1027-1045, 2021.
8. Yuan X, Wang E, Xiao X, Wang J, Yang X, Yang P, Li G and Liu Z: The role of IL-25 in the reduction of oxidative stress and the apoptosis of airway epithelial cells with specific immunotherapy in an asthma mouse model. Am J Transl Res 9: 4137-4148, 2017.
9. Potaczek DP, Miethe S, Schindler V, Alhamdan F and Garn H: Role of airway epithelial cells in the development of different asthma phenotypes. Cell Signal 69: 109523, 2020.
10. Ngo V and Duennwald ML: Nrf2 and oxidative stress: A general overview of mechanisms and implications in human disease. Antioxidants (Basel) 11: 2345, 2022.
11. Ahmed SA and Mohammed WI: Carvedilol induces the antiapoptotic proteins Nrf(2) and Bcl(2) and inhibits cellular apoptosis in aluminum-induced testicular toxicity in male Wistar rats. Biomed Pharmacother 139: 111594, 2021.
12. Liu Q, Gao Y and Ci X: Role of Nrf2 and its activators in respiratory diseases. Oxid Med Cell Longev 2019: 7090534, 2019.
13. Helou DG, Noel B, Gaudin F, Groux H, El Ali Z, Pallardy M, Chollet-Martin S and Kerdine-Römer S: Cutting Edge: Nrf2 Regulates neutrophil recruitment and accumulation in skin during contact hypersensitivity. J Immunol 202: 2189-2194, 2019.
14. Shintani Y, Maruoka S, Gon Y, Koyama D, Yoshida A, Kozu Y, Kuroda K, Takeshita I, Tsuboi E, Soda K and Hashimoto S: Nuclear factor erythroid 2-related factor 2 (Nrf2) regulates airway epithelial barrier integrity. Allergol Int 64 (Suppl): S54-S63, 2015.
15. Hu J, Wang J, Li C and Shang Y: Fructose-1,6-bisphosphatase aggravates oxidative stress-induced apoptosis in asthma by suppressing the Nrf2 pathway. J Cell Mol Med 25: 5001-5014, 2021.
16. Sussan TE, Gajghate S, Chatterjee S, Mandke P, McCormick S, Sudini K, Kumar S, Breysse PN, Diette GB, Sidhaye VK and Biswal S: Nrf2 reduces allergic asthma in mice through enhanced airway epithelial cytoprotective function. Am J Physiol Lung Cell Mol Physiol 309: L27-L36, 2015.
17. Zhang JH, Yang X, Chen YP, Zhang JF and Li CQ: Nrf2 Activator RTA-408 Protects Against Ozone-Induced Acute Asthma Exacerbation by Suppressing ROS and γδT17 Cells. Inflammation 42: 1843-1856, 2019.
18. Yamamoto T, Miyata J, Arita M, Fukunaga K and Kawana A: Current state and future prospect of the therapeutic strategy targeting cysteinyl leukotriene metabolism in asthma. Respir Investig 57: 534-543, 2019.
19. Papi A, Brightling C, Pedersen SE and Reddel HK: Asthma. Lancet 391: 783-800, 2018.
20. van der Burg N, Stenberg H, Bjermer L, Diamant Z and Tufvesson E: Cysteinyl-leukotriene and prostaglandin pathways in bronchial versus alveolar lavage in allergic asthmatics. Allergy 77: 2549-2551, 2022.
21. Ban GY, Kim SH and Park HS: Persistent eosinophilic inflammation in adult asthmatics with high serum and urine levels of leukotriene E(4). J Asthma Allergy 14: 1219-1230, 2021.
22. Polomska J, Bar K and Sozanska B: Exhaled Breath Condensate-A non-invasive approach for diagnostic methods in asthma. J Clin Med 10: 2697, 2021.
23. da Cunha AA, Silveira JS, Antunes GL, Abreu da Silveira K, Benedetti Gassen R, Vaz Breda R and Márcio Pitrez P: Cysteinyl leukotriene induces eosinophil extracellular trap formation via cysteinyl leukotriene 1 receptor in a murine model of asthma. Exp Lung Res 47: 355-367, 2021.
24. Israel E, Chervinsky PS, Friedman B, Van Bavel J, Skalky CS, Ghannam AF, Bird SR and Edelman JM: Effects of montelukast and beclomethasone on airway function and asthma control. J Allergy Clin Immunol 110: 847-854, 2002.
25. Quaranta VN, Dragonieri S, Crimi N, Crimi C, Santus P, Menzella F, Pelaia C, Scioscia G, Caruso C, Bargagli E, *et al*: Can leukotriene receptor antagonist therapy improve the control of patients with severe asthma on biological therapy and coexisting bronchiectasis? A Pilot Study. J Clin Med 11: 4702, 2022.
26. Miyata J, Fukunaga K, Kawashima Y, Ohara O and Arita M: Cysteinyl leukotriene metabolism of human eosinophils in allergic disease. Allergol Int 69: 28-34, 2020.
27. Meshram D, Bhardwaj K, Rathod C, Mahady GB and Soni KK: The role of leukotrienes inhibitors in the management of chronic inflammatory diseases. Recent Pat Inflamm Allergy Drug Discov 14: 15-31, 2020.
28. Dholia N, Sethi GS, Naura AS and Yadav UCS: Cysteinyl leukotriene D(4) (LTD(4)) promotes airway epithelial cell inflammation and remodelling. Inflamm Res 70: 109-126, 2021.

29. Chen X, Peng W, Zhou R, Zhang Z and Xu J: Montelukast improves bronchopulmonary dysplasia by inhibiting epithelial-mesenchymal transition via inactivating the TGF-β1/Smads signaling pathway. Mol Med Rep 22: 2564-2572, 2020.
30. Du C, Zhang Q, Wang L, Wang M, Li J and Zhao Q: Effect of montelukast sodium and graphene oxide nanomaterials on mouse asthma model. J Nanosci Nanotechnol 21: 1161-1168, 2021.
31. Fei X, Zhang X, Zhang GQ, Bao WP, Zhang YY, Zhang M and Zhou X: Cordycepin inhibits airway remodeling in a rat model of chronic asthma. Biomed Pharmacother 88: 335-341, 2017.
32. Bai F, Fang L, Hu H, Yang Y, Feng X and Sun D: Vanillic acid mitigates the ovalbumin (OVA)-induced asthma in rat model through prevention of airway inflammation. Biosci Biotechnol Biochem 83: 531-537, 2019.
33. Bianchi M and Panerai AE: Anti-hyperalgesic effects of tramadol in the rat. Brain Res 797: 163-166, 1998.
34. Costa PPC, Waller SB, Dos Santos GR, Gondim FL, Serra DS, Cavalcante FSÁ, Gouveia Júnior FS, de Paula Júnior VF, Sousa EHS, Lopes LGF, *et al*: Anti-asthmatic effect of nitric oxide metallo-donor FOR811A [cis-[Ru(bpy)2(2-MIM)(NO)](PF6)3] in the respiratory mechanics of Swiss mice. PLoS One 16: e0248394, 2021.
35. Jurisic V: Multiomic analysis of cytokines in immuno-oncology. Expert Rev Proteomics 17: 663-674, 2020.
36. Livak KJ and Schmittgen TD: Analysis of relative gene expression data using real-time quantitative PCR and the 2(-Delta Delta C(T)) Method. Methods 25: 402-408, 2001.
37. Vuletic A, Konjevic G, Milanovic D, Ruzdijic S and Jurisic V: Antiproliferative effect of 13-cis-retinoic acid is associated with granulocyte differentiation and decrease in cyclin B1 and Bcl-2 protein levels in G0/G1 arrested HL-60 cells. Pathol Oncol Res 16: 393-401, 2010.
38. Jurisic V, Srdic-Rajic T, Konjevic G, Bogdanovic G and Colic M: TNF-alpha induced apoptosis is accompanied with rapid CD30 and slower CD45 shedding from K-562 cells. J Membr Biol 239: 115-122, 2011.
39. Thornton CA, Holloway JA, Popplewell EJ, Shute JK, Boughton J and Warner JO: Fetal exposure to intact immunoglobulin E occurs via the gastrointestinal tract. Clin Exp Allergy 33: 306-311, 2003.
40. Alobaidi AH, Alsamarai AM and Alsamarai MA: Inflammation in asthma pathogenesis: Role of T cells, macrophages, epithelial cells and type 2 inflammation. Antiinflamm Antiallergy Agents Med Chem 20: 317-332, 2021.
41. Zeki AA, Bratt JM, Rabowsky M, Last JA and Kenyon NJ: Simvastatin inhibits goblet cell hyperplasia and lung arginase in a mouse model of allergic asthma: A novel treatment for airway remodeling? Transl Res 156: 335-349, 2010.
42. Yamauchi K and Inoue H: Airway remodeling in asthma and irreversible airflow limitation-ECM deposition in airway and possible therapy for remodeling. Allergol Int 56: 321-329, 2007.
43. Poprac P, Jomova K, Simunkova M, Kollar V, Rhodes CJ and Valko M: Targeting free radicals in oxidative stress-related human diseases. Trends Pharmacol Sci 38: 592-607, 2017.
44. Pandey V, Yadav V, Singh R, Srivastava A and Subhashini: β-Endorphin (an endogenous opioid) inhibits inflammation, oxidative stress and apoptosis via Nrf-2 in asthmatic murine model. Sci Rep 13: 12414, 2023.
45. Ozdermir C, Kucuksezer UC, Ogulur I, Pat Y, Yazici D, Ardicli S, Akdis M, Nadeau K and Akdis CA: Lifestyle changes and industrialization in the development of allergic diseases. Curr Allergy Asthma Rep 24: 331-345, 2024.
46. Agache I, Eguiluz-Gracia I, Cojanu C, Laculiceanu A, Del Giacco S, Zemelka-Wiacek M, Kosowska A, Akdis CA and Jutel M: Advances and highlights in asthma in 2021. Allergy 76: 3390-3407, 2021.
47. Patel SJ and Teach SJ: Asthma. Pediatr Rev 40: 549-567, 2019.
48. Kumar RK, Herbert C and Foster PS: The 'classical' ovalbumin challenge model of asthma in mice. Curr Drug Targets 9: 485-494, 2008.
49. Nakagome K and Nagata M: Involvement and possible role of eosinophils in asthma exacerbation. Front Immunol 9: 2220, 2018.
50. Garcia G, Taille C, Laveneziana P, Bourdin A, Chanez P and Humbert M: Anti-interleukin-5 therapy in severe asthma. Eur Respir Rev 22: 251-257, 2013.
51. Price DB, Rigazio A, Campbell JD, Bleecker ER, Corrigan CJ, Thomas M, Wenzel SE, Wilson AM, Small MB, Gopalan G, *et al*: Blood eosinophil count and prospective annual asthma disease burden: A UK cohort study. Lancet Respir Med 3: 849-858, 2015.
52. Ying S, Meng Q, Zeibecoglou K, Robinson DS, Macfarlane A, Humbert M and Kay AB: Eosinophil chemotactic chemokines (eotaxin, eotaxin-2, RANTES, monocyte chemoattractant protein-3 (MCP-3), and MCP-4), and C-C chemokine receptor 3 expression in bronchial biopsies from atopic and nonatopic (Intrinsic) asthmatics. J Immunol 163: 6321-6329, 1999.
53. Poowuttikul P, Saini S and Seth D: Inner-City Asthma in Children. Clin Rev Allergy Immunol 56: 248-268, 2019.
54. Matucci A, Vultaggio A, Maggi E and Kasujee I: Is IgE or eosinophils the key player in allergic asthma pathogenesis? Are we asking the right question? Respir Res 19: 113, 2018.
55. Kanaoka Y and Boyce JA: Cysteinyl leukotrienes and their receptors: Cellular distribution and function in immune and inflammatory responses. J Immunol 173: 1503-1510, 2004.
56. Zhou X, Cai J, Liu W, Wu X and Gao C: Cysteinyl leukotriene receptor type 1 (CysLT1R) antagonist zafirlukast protects against TNF-α-induced endothelial inflammation. Biomed Pharmacother 111: 452-459, 2019.
57. Patel B, Gupta N and Ahsan F: Aerosolized montelukast polymeric particles-an alternative to oral montelukast-alleviate symptoms of asthma in a rodent model. Pharm Res 31: 3095-3105, 2014.
58. Basyigit I, Sahin M, Sahin D, Yildiz F, Boyaci H, Sirvanci S and Ercan F: Anti-inflammatory effects of montelukast on smoke-induced lung injury in rats. Multidiscip Respir Med 5: 92-98, 2010.
59. Wu AY, Chik SC, Chan AW, Li Z, Tsang KW and Li W: Anti-inflammatory effects of high-dose montelukast in an animal model of acute asthma. Clin Exp Allergy 33: 359-366, 2003.
60. Wu Y, Zhou C, Tao J and Li S: Montelukast prevents the decrease of interleukin-10 and inhibits NF-kappaB activation in inflammatory airway of asthmatic guinea pigs. Can J Physiol Pharmacol 84: 531-537, 2006.
61. Abdel Aziz RR, Helaly NY, Zalata KR and Gameil NM: Influence of inhaled beclomethasone and montelukast on airway remodeling in mice. Inflammopharmacology 21: 55-66, 2013.
62. Holgate ST, Peters-Golden M, Panettieri RA and Henderson WR Jr: Roles of cysteinyl leukotrienes in airway inflammation, smooth muscle function, and remodeling. J Allergy Clin Immunol 111 (1 Suppl): S18-S34; discussion S34-16, 2003.
63. Berair R, Hartley R, Mistry V, Sheshadri A, Gupta S, Singapuri A, Gonem S, Marshall RP, Sousa AR, Shikotra A, *et al*: Associations in asthma between quantitative computed tomography and bronchial biopsy-derived airway remodelling. Eur Respir J 49: 1601507, 2017.
64. Jurisic V, Bogdanovic G, Kojic V, Jakimov D and Srdic T: Effect of TNF-alpha on Raji cells at different cellular levels estimated by various methods. Ann Hematol 85: 86-94, 2006.
65. Jurisic V, Terzic T, Colic S and Jurisic M: The concentration of TNF-alpha correlate with number of inflammatory cells and degree of vascularization in radicular cysts. Oral Dis 14: 600-605, 2008.
66. Jurisic V, Bumbasirevic V, Konjevic G, Djuricic B and Spuzic I: TNF-alpha induces changes in LDH isotype profile following triggering of apoptosis in PBL of non-Hodgkin's lymphomas. Ann Hematol 83: 84-91, 2004.
67. Michaeloudes C, Abubakar-Waziri H, Lakhdar R, Raby K, Dixey P, Adcock IM, Mumby S, Bhavsar PK and Chung KF: Molecular mechanisms of oxidative stress in asthma. Mol Aspects Med 85: 101026, 2022.
68. Audousset C, McGovern T and Martin JG: Role of Nrf2 in Disease: Novel molecular mechanisms and therapeutic approaches-pulmonary disease/asthma. Front Physiol 12: 727806, 2021.
69. Yachie A: Heme oxygenase-1 deficiency and oxidative stress: A review of 9 independent human cases and animal models. Int J Mol Sci 22: 1514, 2021.
70. Ross D and Siegel D: The diverse functionality of NQO1 and its roles in redox control. Redox Biol 41: 101950, 2021.